JSEE Vol. 27, No. 1, 2025 DOI: 10.48303/jsee.2024.2039374.1121

Research Paper

Numerical Investigation of the Influence of Seismic Excitation Characteristics on the Response of Hunchbacked Block-Type Quay Walls with Varying Geometries

Ali Akbar Ehterami[1], Babak Ebrahimian[2*] and Ali Noorzad[3]

1. Ph.D. Candidate, Faculty of Civil, Water and Environmental Engineering, Shahid Beheshti University (SBU), Tehran, Iran
2. Assistant Professor, Faculty of Civil, Water and Environmental Engineering, Shahid Beheshti University (SBU), Tehran, Iran, *Corresponding Author; email: b_ebrahimian@sbu.ac.ir
3. Professor, Faculty of Civil, Water and Environmental Engineering, Shahid Beheshti University (SBU), Tehran, Iran

Received: 23/08/2024
Revised: 24/09/2024
Accepted: 08/10/2024

Keywords:
Hunchbacked quay wall; Seismic performance; Performance-based design; Nonlinear dynamic analysis; Soil-structure interaction; 1g shaking table

ABSTRACT

Using the finite element method, this study investigates the seismic behavior of hunchbacked block-type gravity quay walls with varying configurations. The research employs adaptive meshing strategies and error-based adaptivity techniques to refine the plane strain FE meshes. Interface elements are utilized to simulate discontinuities along the wall height, particularly between concrete blocks, and to model the interaction between the quay wall and the adjacent soil medium. The developed FE models are validated against data from 1g shaking table tests available in the literature. The study evaluates the seismic performance of three quay wall models, each with a unique configuration, under a range of seismic loads, including peak ground accelerations from 0.1g to 0.9g and frequencies from 3.0 Hz to 9.0 Hz. The findings indicate that increasing hunch height and optimizing the upper inclination angle effectively reduce lateral earth pressures and horizontal displacements, enhancing seismic performance. The study recommends positioning critical structures, infrastructure, and sensitive buildings in the backfill area at a distance greater than the wall height, as maximum backfill settlement occurs between 0.55H and 0.65H from the quay wall, where significant settlement poses risks to facilities. Additionally, acceleration amplification in the backfill decreases at distances greater than the wall height, indicating reduced seismic impact.

How to cite the article:
Ehterami, A. A., Ebrahimian, B., & Noorzad, A. (2025). Numerical Investigation of the Influence of Seismic Excitation Characteristics on the Response of Hunchbacked Block-Type Quay Walls with Varying Geometries. *Journal of Seismology and Earthquake Engineering*, *27*(1), 1-21. doi: 10.48303/jsee.2024.2039374.1121

1. Introduction

Ports are essential to the global marine transportation network, significantly influencing the development of coastal areas. Quay walls, critical waterfront structures within port infrastructure, are crucial for facilitating import and export activities. However, these structures are susceptible to seismic risks (Chen et al., 2024a; Ko et al., 2024). Gravity-type quay walls, which run parallel to the shoreline, are coastal structures designed to retain backfill soil. They are usually built on a rubble mound foundation layer to distribute loads to the seabed soil, fulfilling bearing capacity and stability requirements (Guo et al., 2023). These walls provide a deep vertical face for vessel approach, docking, and operations.

Historically, gravity quay walls have experienced severe damage during earthquakes. The primary causes of damage during seismic activity include differential settlement of the backfill and ground distortion. For instance, during the 1986 Kalamata earthquake in Greece, block-type quay walls at Kalamata Port tilted towards the sea by 4 to 5 degrees, despite their robust foundation. Similarly, the 1995 Kobe earthquake in Japan caused quay walls at Port Island to sink and shift towards the sea, resulting in backfill soil settlement of up to 2.0 m and a maximum horizontal displacement of 5.0 m (Ishihara et al., 1996; Iai, 2019). The 1995 Kobe earthquake resulted in varying degrees of damage to industrial structures and storage tanks. The 1999 Chi-Chi earthquake in Taiwan affected Taichung Harbor, where quay walls moved approximately 1.7 m towards the sea, leading to substantial vertical settlements, cracks, and permanent shifts in the service area behind the walls, with backfill settlements recorded up to 0.94 m, causing infrastructure destruction (Lee, 2005). Other significant events include the 1999 Kocaeli earthquake, impacting Ergil and Esenkoy Ports (Yuksel et al., 2017). The 2011 Tohoku earthquake in Japan, the most powerful earthquake recorded in the country, exposed significant design and construction flaws in quay walls, leading to widespread structural failures and underscoring the need for improved engineering practices to withstand extreme seismic events (Sugano et al., 2014). The 2018 Taiwan earthquake also impacted the structures of Hualien port (Ko et al., 2024).

The seismic behavior and the vulnerability of gravity-type quay walls are studied using both numerical (Tiznado and Rodriguez-Roa, 2011; Arablouei et al., 2011; Ebrahimian, 2013; Khosrojerdi and Pak, 2015; Tong and Schaefer, 2016; Dakoulas et al., 2018; Tong et al., 2018; Jafarian and Miraei, 2019; Ebrahimian and Bahmani, 2019; Shekari, 2023; Chen et al., 2024a) and experimental (Moghadam et al., 2009, 2011; Chakraborty and Choudhury, 2014; Yuksel et al., 2017; Santhoshkumar, 2020; Ghalandarzadeh et al., 2020; Lee et al., 2022; Guo et al., 2023) approaches, leading to a comprehensive understanding of these critical infrastructure components. Most of these studies focus on caisson-type quay walls. However, the seismic response of block-type quay walls, the most basic form of gravity wall constructed with concrete or natural stone blocks, has received less attention (Calabrese and Lai, 2016; Ehterami et al., 2024). These walls are suitable for firm and well-bearing subsoils and are particularly susceptible to overturning, requiring specific damage criteria (PIANC, 2001; Cihan et al., 2015; and Ebrahimian and Farahani, 2024).

Traditional seismic design methods often fail to capture the complexities inherent in block-type quay walls, as they rely on simplifications that can lead to prediction and estimation errors (Dakoulas et al., 2018; Cihan and Cihan, 2021). Conventionally, seismic design codes for waterfront retaining structures use a force balance approach. However, the International Navigation Association advocates for a performance-based design method for quay structures that considers damage levels based on residual horizontal displacement and the seaward rotation angle of gravity-type quay walls (PIANC, 2001).

A landward-leaning quay wall can reduce the failure wedge and lateral earth pressure resistance compared to a vertical wall but at a significantly higher cost (Sadrekarimi et al., 2008). The hunchbacked wall configuration, which benefits from reduced lateral soil pressure, can mitigate costs, weight, and volume while enhancing seismic resilience, as demonstrated by Sadrekarimi (2011, 2012) through 1 g shaking table model experiments. Fragility curves for hunchbacked block-type quay walls are developed based on numerical simulations by Alielahi and Rabeti Moghadam (2016). Further studies have

indicated that a high relative density seabed foundation can decrease quay wall settlements and rotation, although block-to-block sliding can still cause horizontal displacements (Dakoulas et al., 2018). Comparative studies of vertical and hunchbacked block-type quay walls by Yuksel et al. (2017, 2023) show that a hunchbacked wall with a lower breaking point has better seismic performance due to its lower center of gravity, reducing overturning moments. The effectiveness of base block inclination in reducing horizontal displacement of hunchbacked quay walls is investigated by Baziar et al. (2020). A numerical model to determine the optimal hunch angle for a hunchbacked block-type quay wall is developed by Ebrahimian and Farahani (2023a), using multiple linear regression and machine learning algorithms to estimate the optimal angle. The study by Ehterami et al. (2024) indicates that hunchbacked quay walls with higher breaking points are more prone to sliding and rotating landward, while those with lower breaking points tend to slide and rotate seaward, posing a greater risk of overturning or collapsing in concrete block-type walls.

This study specifically examines the impact of variations in hunch height (H_h) and upper inclination angle (θ_i), while keeping the hunch angle (ω_i) constant, on the seismic performance of quay walls. Figure (1) depicts three distinct hunchbacked

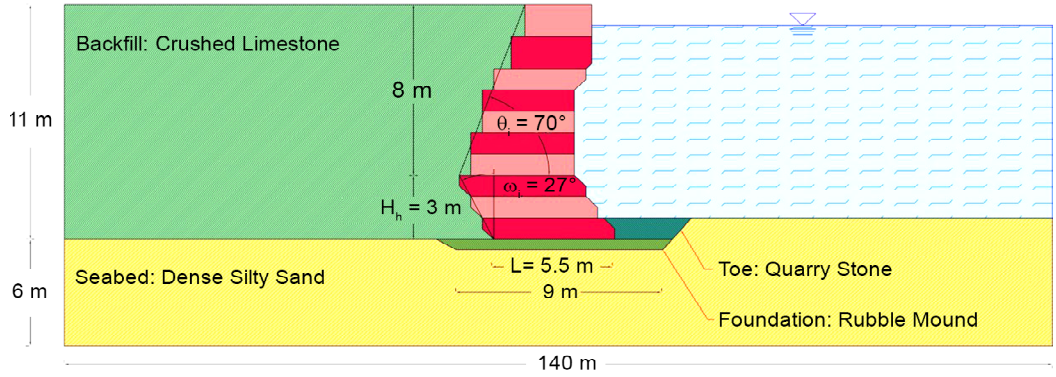

(a) QW-I (Sadrekarimi, 2011, 2012)

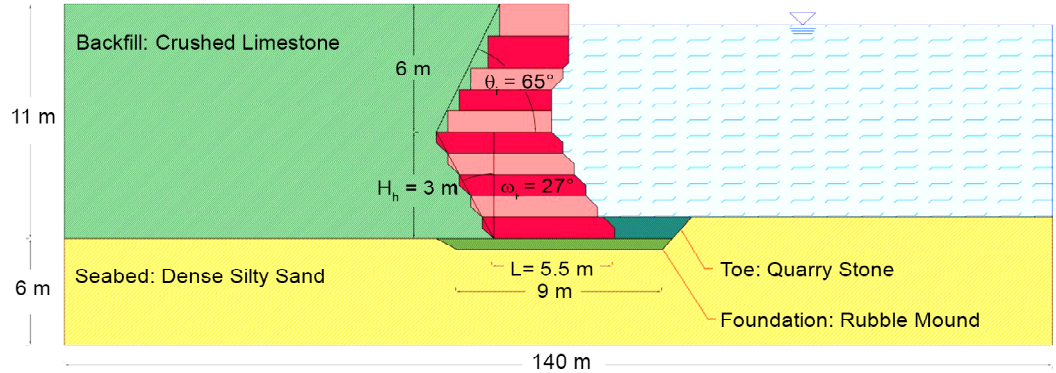

(b) QW-II

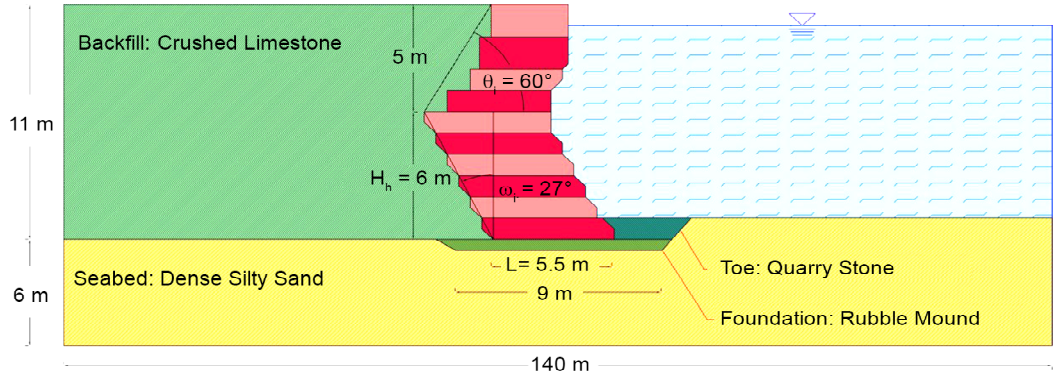

(c) QW-III

Figure 1. Geometry of considered hunchbacked block-type quay walls.

block-type quay walls. Building on the 1 g shaking table tests by Sadrekarimi (2011, 2012), the current numerical study employs the same experimental models for validation. The validation process uses the finite element method, incorporating nonlinear time history analysis and the HSsmall constitutive model. After calibrating model parameters, the research adopts a comprehensive approach. The study investigates the effects of different seismic loads characterized by varying peak ground accelerations (PGA) ranging from 0.1 g to 0.9 g, as well as frequencies spanning 3.0 Hz to 9.0 Hz on quay walls.

2. Numerical Modeling Procedure

The FEM is utilised to evaluate the impact of block configuration, soil properties, and foundation stiffness on the performance of quay walls. Numerous studies have demonstrated the effectiveness of FEM in predicting the seismic response of quay walls (Augarde et al., 2021; Yuksel et al., 2023; Chen et al., 2024a; Liu et al., 2024; Ehterami et al., 2024). Accurate modelling within FEM requires the appropriate selection of boundary conditions, constitutive laws, and contact interactions (Rezaei Farei and Ehterami, 2018). In this study, the Midas GTS NX software (MIDAS IT Co. Ltd., 2021) is employed for nonlinear dynamic time history analyses to investigate the seismic behaviour of hunchbacked block-type gravity quay walls. The software effectively simulates soil-structure interactions, foundation design, and slope stability using advanced material modelling features (Niu et al., 2024; Savigamin and Bobet, 2024; Soltani-Jigheh and Ehterami, 2024).

A critical step in FEM is mesh construction, which divides the problem domain into finite elements (Rezaei Farei and Ehterami, 2019). Mesh refinement enhances resolution and accuracy, particularly in areas with significant changes or errors (Alimoradi et al., 2024). This study employs a hybrid approach that integrates adaptive meshing (Stelzer and Hofstetter, 2005; Kardani et al., 2011; Mezeh et al., 2018) with error-based adaptivity techniques (Radampola et al., 2008; Mroginski and Etse, 2013) to automatically construct and refine two-dimensional plane strain meshes. Precise data from 1 g shaking table tests conducted by Sadrekarimi (2011, 2012) is used as a benchmark to identify the most accurate mesh configuration. A comprehensive adaptivity plan is formulated to optimise mesh configurations for simulations. The Midas GTS NX meshing generator is utilised for accurately and efficiently simulating soil-structure interactions, capable of creating Delaunay triangulations, constrained Delaunay triangulations, and Voronoi diagrams, which expedite the meshing process (Zhang et al., 2022). Validation models and mesh convergence studies reveal that the optimal numerical solutions are achieved by combining Delaunay triangular meshes with dimensions of 0.27 m and 0.86 m, as depicted in Figure (2).

Selecting an effective constitutive model is essential for accurately replicating seismic performance. In this study, the HSsmall model is chosen for materials, offering a detailed representation of behaviour under seismic loading (Onyelowe et al., 2023; Alzabeebee and Keawsawasvong, 2023). The HSsmall model extends the basic Hardening Soil (HS) model by incorporating additional parameters to account for the soil's elastic hysteresis behaviour at low strains. This model employs the shear modulus reduction curve proposed by Hardin and Drnevich (1972) and includes parameters such as the initial shear modulus (G_0) and the threshold shear strain ($\gamma_{0.7}$). In this study, a value of $\gamma_{0.7} = 0.016$ is selected based on curves suggested by Seed et al. (1986) and Sadrekarimi (2012) for sandy seabed and gravelly backfill, aligning with the findings of Bajaj and Anbazhagan (2019) considering the soil type used in this research. The stiffness dependency on the stress level in the HSsmall model is determined by effective stress and strength parameters. This relationship is described by an equation involving the reference initial shear modulus (G_0^{ref}) at a reference pressure P^{ref} of 100 kPa, the minimum principal effective stress (σ'_3), and a constant parameter (m) governing the stress dependency (Equation 1). Similar equations define other stiffness parameters such as the loading-unloading stiffness E_{ur}^{ref} (Equation 2), the secant stiffness in the drained triaxial test E_{50}^{ref} (Equation 3), and the tangent stiffness for initial oedometer loading E_{oed}^{ref} (Equation 4) (Xiao et al., 2024; Goyal and Shrivastava, 2024).

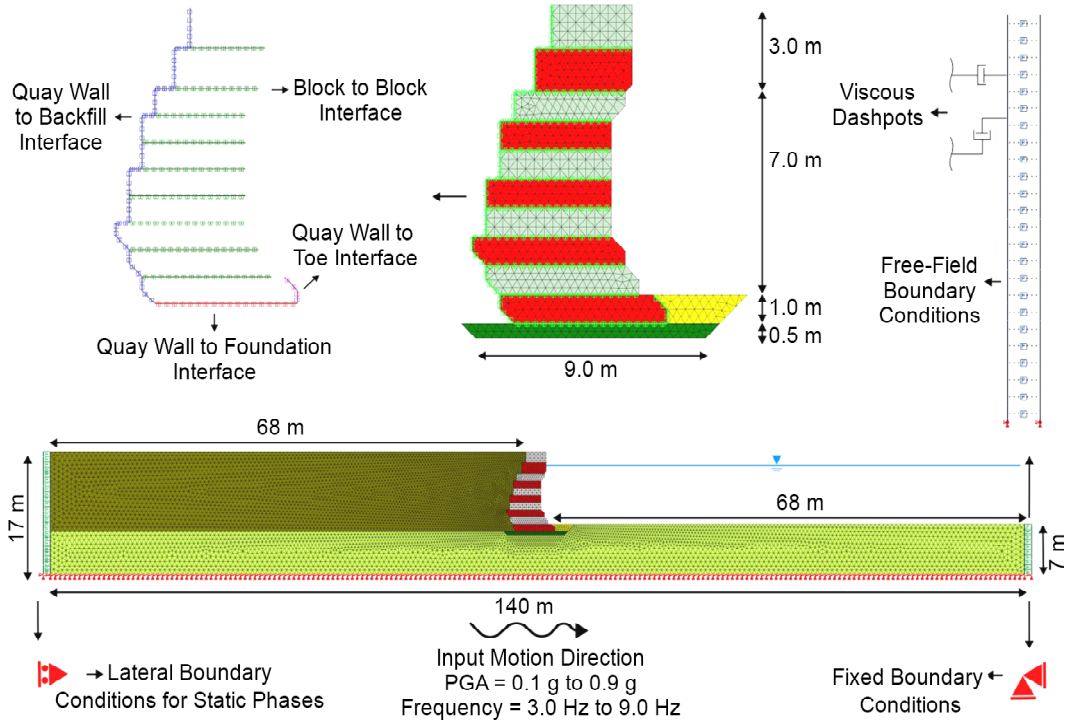

Figure 2. Developed numerical model.

Table 1. Material and interface properties for different sections of the developed FE model.

Material	e_{max}	e_{min}	υ	K (cm/s)	φ (deg)	ψ (deg)	γ (kN/m^3)	γ_{sat} (kN/m^3)	m	$E_{50}^{ref} - E_{oed}^{ref}$ (kN/m^2)	E_{ur}^{ref} (kN/m^2)
Concrete Block	-	-	0.2	-	-	-	21.00	-	-	20×10^6	-
Foundation	0.96	0.69	0.3	32	36	6	16.63	19.76	0.5	12×10^4	36×10^4
Toe	0.96	0.71	0.3	63	35	7	16.02	19.64	0.5	10×10^4	30×10^4
Seabed	0.94	0.61	0.3	0.012	36	6	16.95	20.07	0.5	19×10^4	57×10^4
Backfill	0.96	0.67	0.3	50	38	1	17.59	19.59	0.5	11×10^4	33×10^4

	Location	k_n (kN/m^3)	k_t (kN/m^3)	φ (deg)
Interface Elements	Block to Toe	4.8×10^6	4.3×10^5	23.64
	Block to Block	5.4×10^8	4.9×10^7	10.00
	Block to Backfill	2.3×10^6	2.1×10^5	17.31
	Block to Foundation	8.9×10^6	8.1×10^5	23.62

$$G_0 = G_0^{ref}\left(\frac{c'\cos\varphi' + \sigma_3'\sin\varphi'}{c'\cos\varphi' + p^{ref}\sin\varphi'}\right)^m \quad (1)$$

$$E_{50} = E_{50}^{ref}\left(\frac{c\cos\varphi + \sigma_3'\sin\varphi}{c\cos\varphi + p^{ref}\sin\varphi}\right)^m \quad (2)$$

$$E_{oed} = E_{oed}^{ref}\left(\frac{c\cos\varphi + \sigma_3'\sin\varphi}{c\cos\varphi + p^{ref}\sin\varphi}\right)^m \quad (3)$$

$$E_{ur} = E_{ur}^{ref}\left(\frac{c\cos\varphi + \sigma_3'\sin\varphi}{c\cos\varphi + p^{ref}\sin\varphi}\right)^m \quad (4)$$

The numerical model developed for this study uses laboratory test data from Sadrekarimi (2011, 2012). Table (1) outlines the parameters and corresponding soil properties. By comparing the numerical model's outcomes with laboratory results, the accuracy of the employed methodology is verified, allowing for the precise estimation of soil constitutive parameters. This ensures an accurate representation of soil response to dynamic loads and facilitates the analysis of the quay wall's dynamic behaviour, accounting for soil-structure interaction.

The interface elements in a discontinuous gravity-type hunchbacked quay wall system typically consist of two main components: (I) quay wall to soil and (II) block-to-block connections. The quay wall-to-soil interface employs various elements tailored to specific modelling requirements (Ebrahimian and Bauer, 2012).

Common options include a contact interface element that allows sliding and separation (Yu et al., 2015) or an interface element with discontinuities that treats the soil and wall as distinct materials (Cihan et al., 2015). Soil properties significantly affect the behaviour of this interface, capturing nonlinear soil behaviour (Ebrahimian et al., 2012; Ebrahimian and Bauer, 2014), while wall geometry influences load and stress distribution. For block-to-block interfaces, the Coulomb frictional model is frequently employed (Yuksel et al., 2023). This model assumes that the frictional resistance between adjacent blocks is directly proportional to the normal force acting on them (Coutinho et al., 2003). This relationship is crucial for accurately simulating shear resistance and sliding behavior, particularly during dynamic loading events such as seismic activities, where blocks may experience significant relative movement.

In this study, to replicate the tangential behaviour between the quay wall and surrounding soils as well as block-to-block contact, normal (k_n) and shear (k_t) springs utilise Coulomb's law of friction with the resistance reduction factor (R_{inter}) (Shabani et al., 2022; Soltani-Jigheh and Ehterami, 2024; Barron et al., 2024). The interface element's properties are adjusted based on numerical models validated against the 1 g shaking table tests conducted by Sadrekarimi (2012). The numerical models are most accurately calibrated with a resistance reduction factor of 0.7 (Zalachoris et al., 2021; Chen et al., 2022; Ehterami et al., 2022), and the characteristics of the interfaces are given in Table (1).

In this study, distinct approaches are employed to impose static and dynamic boundary conditions in the computation process. During the static phase, the bottom boundary is fixed in all directions, while the lateral boundaries are restrained horizontally. In contrast, during the dynamic stage, a rigid foundation is assumed to apply ground acceleration forces, and free boundary conditions are implemented along the vertical sides to prevent wave reflections (Jimenez et al., 2019). Free field boundary conditions are critical for accurately evaluating a soil-structure system subjected to seismic loads, as they replicate the surrounding free field motion that would exist in the absence of the structure. In Midas GTS NX, free-field boundaries along the model's vertical sides fulfill this requirement by allowing for the dissipation of wave energy, thus preventing unrealistic reflections that could distort the analysis.

The configuration illustrated in Figure (2) consists of plane grids connected to the primary grid by viscous dashpots, simulating an infinite ground. This arrangement functions as a quiet boundary, effectively mitigating disturbances caused by plane waves. The viscous dashpots absorb outgoing wave energy, ensuring that the dynamic response of the model accurately reflects the seismic input. The implementation of free field boundaries facilitates one-way coupling, where the behavior of the free field influences the response of the main model without reciprocal interaction. This is particularly important when the free-field elements are positioned at a sufficient distance from the center of the finite element domain, allowing for realistic modeling of seismic effects without complications from boundary reflections. Overall, the use of free field boundary conditions is essential in dynamic finite element analysis, as it enhances the accuracy of the simulation by properly accounting for the motion of the surrounding soil and preventing boundary-induced artifacts in the results.

Rayleigh damping, or proportional damping, is widely used in structural dynamics and earthquake engineering (Timuragaoglu, 2024) and describes energy dissipation due to friction, hysteresis, or other mechanisms in structures or soil subjected to seismic forces. In this study, Rayleigh damping is applied, with the damping matrix derived from the linear combination of the stiffness and mass matrices, represented by Equation (5), where [C] denotes the damping matrix; [M] stands for the mass matrix; [K] represents the stiffness matrix; and α_R and β_R are the damping coefficients. To determine these coefficients, the values of the natural frequencies of two natural vibration modes of the model and the corresponding damping ratios for these modes are derived (Ebrahimian and Panahi, 2019; Haukaas, 2024). Once these values are determined, the coefficients proportional to mass (α_R) and stiffness (β_R) are obtained using Equation (6).

$$[C]=\alpha_R[M]+\beta_R[K] \quad (5)$$

$$\begin{Bmatrix}\alpha_R\\ \beta_R\end{Bmatrix}=\frac{2\xi}{\omega_i+\omega_j}\begin{bmatrix}\omega_i\omega_j\\ 1\end{bmatrix} \quad (6)$$

In this study, the Rayleigh damping ratio (ξ) is set to 5% as the target damping ratio (Fatahi et al., 2020; Yuksel et al., 2023; Ebrahimian and Farahani, 2023b; Ko et al., 2024). Eigenvalue analysis is conducted to determine the primary vibration periods and modes of vibration (Shabani et al., 2022; Ehterami et al., 2024). The most actively participating modes are determined and their time periods are employed in the time history analysis to incorporate damping using the Rayleigh damping method. Following modal eigenvalue analysis with 30 modes on quay wall models, the selected natural frequency values are determined as ω_1=2.96 Hz (18.59 rad/s) and ω_{17}=9.53 Hz (59.87 rad/s), corresponding to α_R=1.418427 and β_R=0.001274 for the QW-I model (Figure 3). Since the values of ω_i and ω_j vary depending on the particular model under consideration, natural frequencies are calculated separately for each quay wall model.

Under varying seismic loads, this study evaluates the behavior of hunchbacked block-type quay walls. The input motion is applied to the model's base using a Gabor wavelet (Gabor, 1946), facilitating a parametric study by systematically varying PGAs and frequencies. This method's computational efficiency allows for a more extensive exploration of the quay wall's response under diverse seismic conditions compared to using numerous real earthquake records. The nonlinear time history analysis investigates how the quay wall behaves under different ground motion conditions, with PGAs ranging from 0.1g to 0.9g and frequencies between 3.0 Hz and 9.0 Hz (Figure 4). These variables encompass seismic characteristics typical of earthquakes in coastal regions worldwide (Towhata, 2021). Additionally, hydrodynamic effects are not considered in this study due to their minimal impact on seawater-structure interaction and the seismic performance of gravity-type quay walls (Arablouei et al., 2011). Previous studies indicate that hydrodynamic effects typically influence the seismic performance of these walls by only about 5% or even less (Gazetas et al., 2016; Dakoulas et al., 2018).

3. Verification

To ensure the accuracy of the FE numerical model and to verify the appropriateness of the constitutive model parameters and boundary conditions, this study utilized data from shaking table tests conducted on hunchbacked gravity block-type quay walls by Sadrekarimi (2011, 2012). The model is subjected to sinusoidal excitations with a PGA of 0.35 g and a frequency of 2.8 Hz. Figure (5c) demonstrates the precisely computed horizontal displacement (D_H) of the quay wall, showing a strong correlation with the observed trends from the experimental tests. Additionally, Figure (5d) illustrates a satisfactory agreement between the numerical simulation and experimental

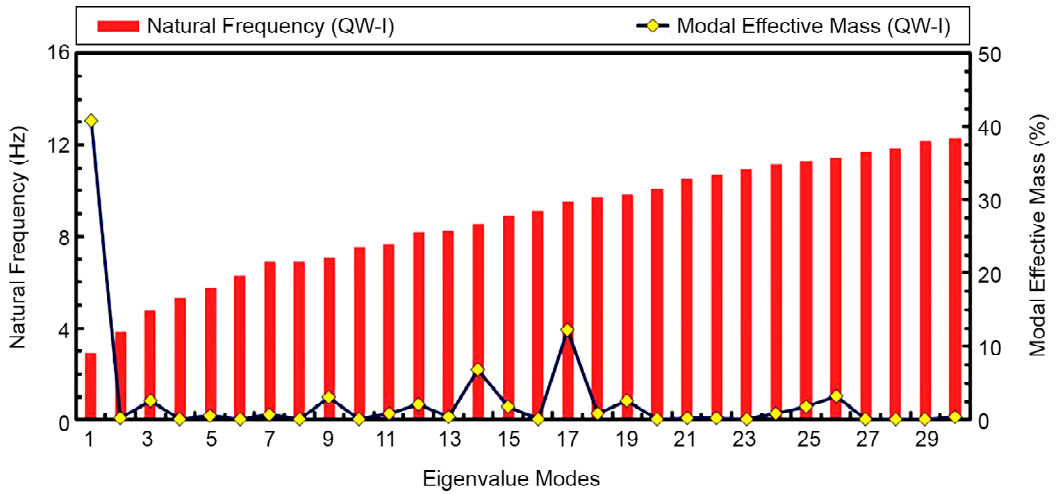

Figure 3. Eigenvalue analysis and natural frequency determination by effective mass.

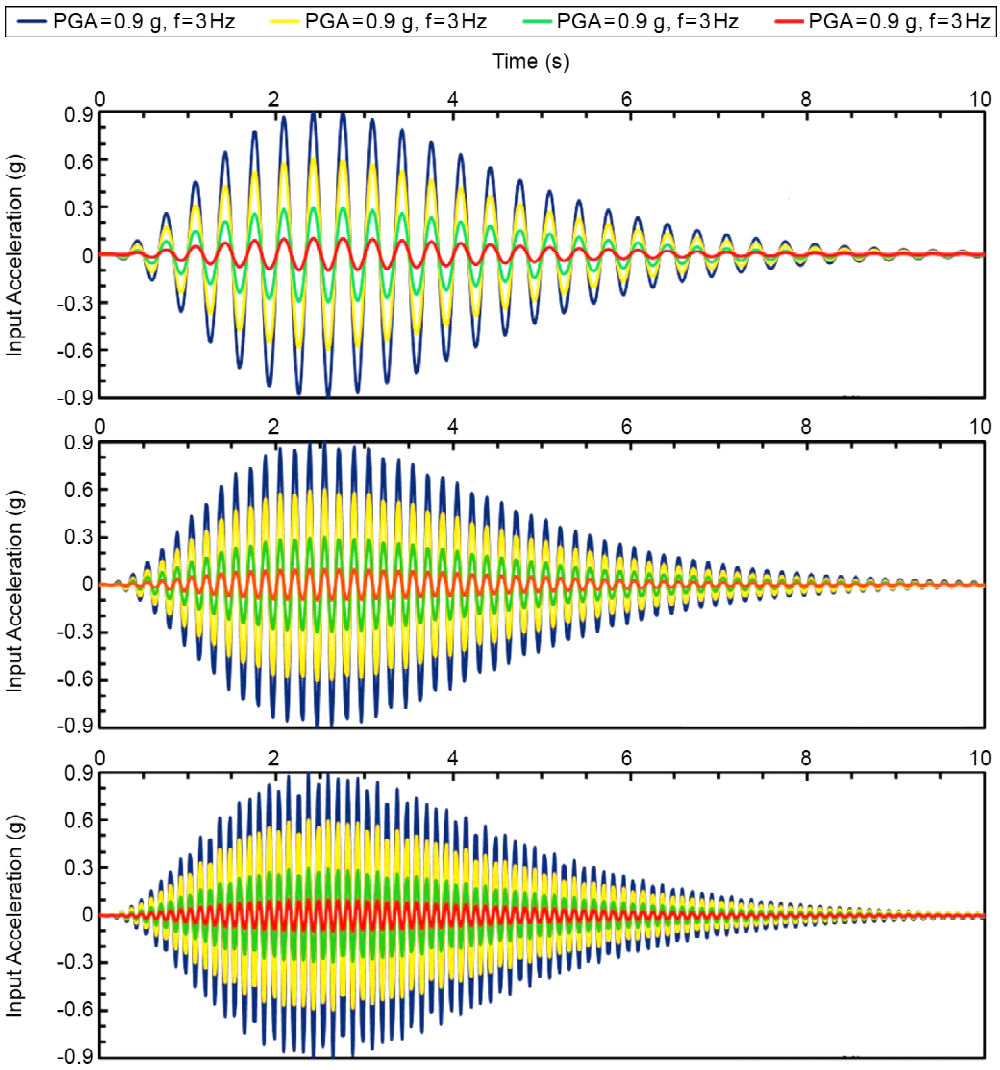

Figure 4. Input acceleration time histories.

results for various measurements, including wall base sliding (S_B) and D_H. Furthermore, the computed total lateral earth pressure (TEP-1) and lateral acceleration (ACC-1) are compared with the numerical model, revealing significant agreements (Figure 5).

4. Results and Discussion

4.1. Quay Wall Displacement

Hunchbacked block-type gravity quay walls are susceptible to displacement under various seismic loading conditions. Figures (6) to (9) illustrate the D_H of the QW-I, QW-II, and QW-III models, and they evaluate each model's dynamic performance based on the criteria outlined by PIANC (2001) for assessing damage levels in gravity-type quay walls. PIANC (2001) has established guidelines for evaluating damage levels for gravity quay walls, considering the normalized residual D_H at the wall head and describing four damage states, representing the conditions of serviceable, repairable, near collapse, and collapse of a gravity quay wall. Additionally, Figures (6) and (7) present results from similar studies conducted by Tasiopoulou et al. (2015) and Yuksel et al. (2017), respectively, for comparison purposes. The QW-I model sustains noticeable damage after 4.32 seconds when subjected to a ground motion with a PGA of 0.9g and a frequency of 3 Hz (Figure 9).

In contrast, the QW-II and QW-III models, which have higher H_h and lower θ_i demonstrate improved dynamic performance. Therefore, increasing H_h and decreasing θ_i lead to decreased D_H and reduced damage to the quay wall. This finding aligns with the results of Alielahi and Rabeti Moghadam (2016) and Yuksel et al. (2017). Notably, under the same dynamic loading conditions, the QW-III model

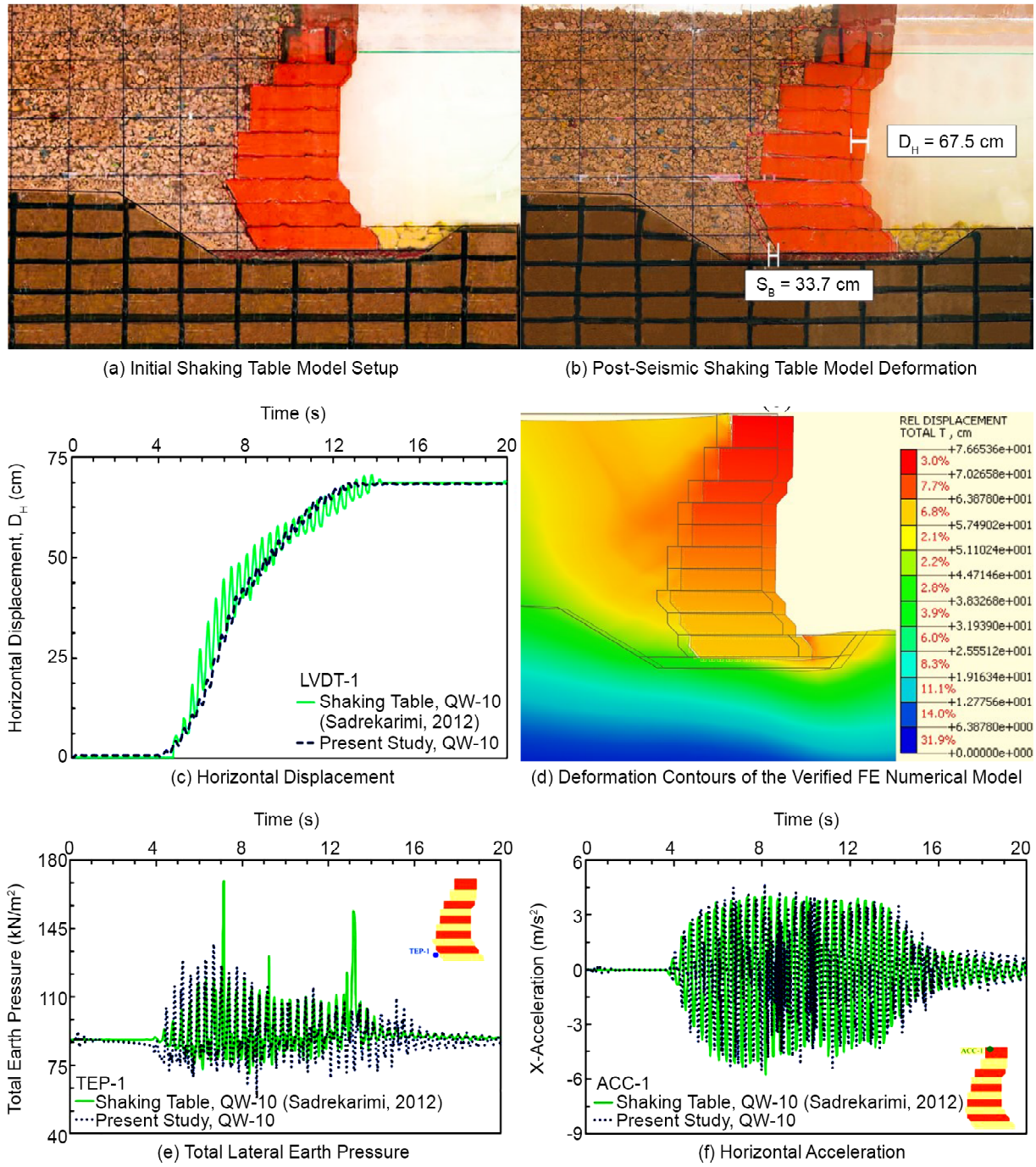

Figure 5. Comparison between the obtained numerical results and the experimental observations (Sadrekarimi, 2011, 2012).

does not experience near-collapse damage levels like the QW-I and QW-II models.

The magnitudes of D_H exhibit a consistent correlation with varying input acceleration levels. Higher acceleration levels correspond to an increase in the quay wall's D_H. Furthermore, reducing the frequency of seismic input motions leads to stronger earthquakes and more critical soil conditions due to several interconnected factors. First, lower-frequency seismic waves tend to carry more energy over longer periods, resulting in greater soil strains and displacement responses that amplify the earthquake's impact (Sandoval and Bobet, 2020).

This increased energy input can cause significant acceleration and displacement responses in structures and related soil mediums, enhancing the destructive potential of the earthquake. Additionally, geotechnical materials often amplify low-frequency seismic waves, which increases the peak acceleration, velocity, and displacement near the surface, leading to more pronounced

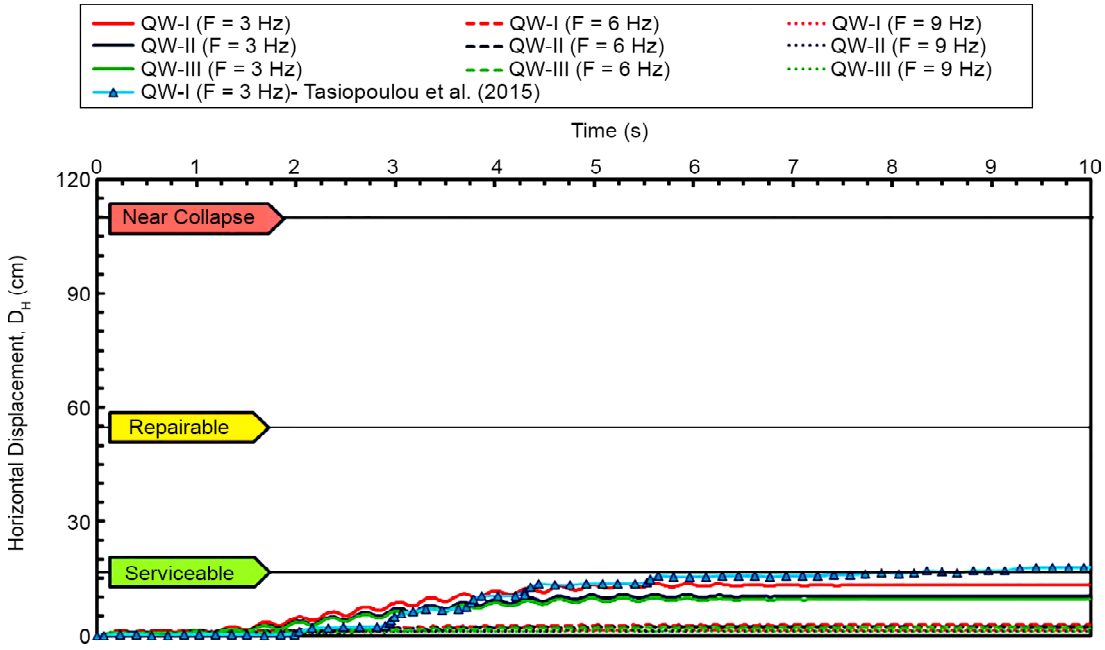

Figure 6. Horizontal displacement time histories of quay walls subjected to an input motion with a PGA = 0.1 g along with an indication of damage levels.

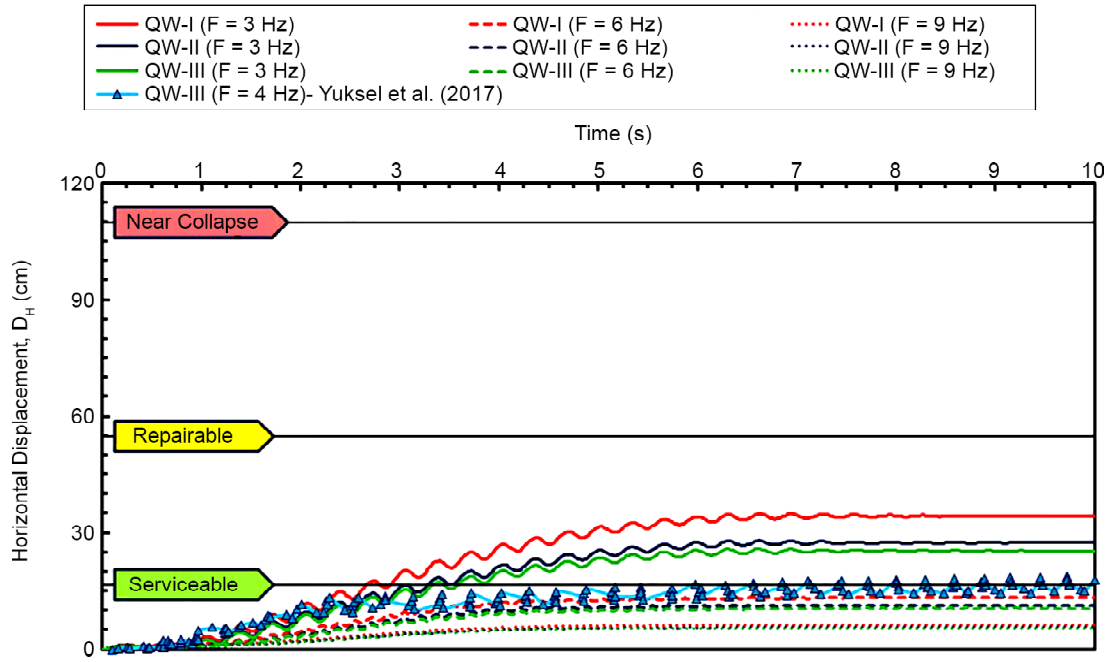

Figure 7. Horizontal displacement time histories of quay walls subjected to an input motion with a PGA = 0.3 g along with an indication of damage levels.

instability and damage (Chen et al., 2024b).

For instance, studies have shown that loess slopes exhibit a strong amplifying effect on low-frequency seismic waves, resulting in greater displacement and potential failure (Li and Mo, 2019). Conversely, the soil often filters out high-frequency seismic waves, thereby reducing their impact. This filtering effect means that the soil absorbs and dissipates the energy of high-frequency waves more effectively, leading to less severe responses compared to low-frequency waves. Various studies have observed this phenomenon, showing that high-frequency components have less influence in causing soil instability and structural damage (Cakir, 2013; Najma and Ghalandarzadeh, 2019; Ha and Kim, 2023). In addition, structures and soil layers have natural frequencies at which they resonate. When the seismic input motion's frequency matches the natural frequency of the structure or soil layer, resonance occurs, resulting in sig-

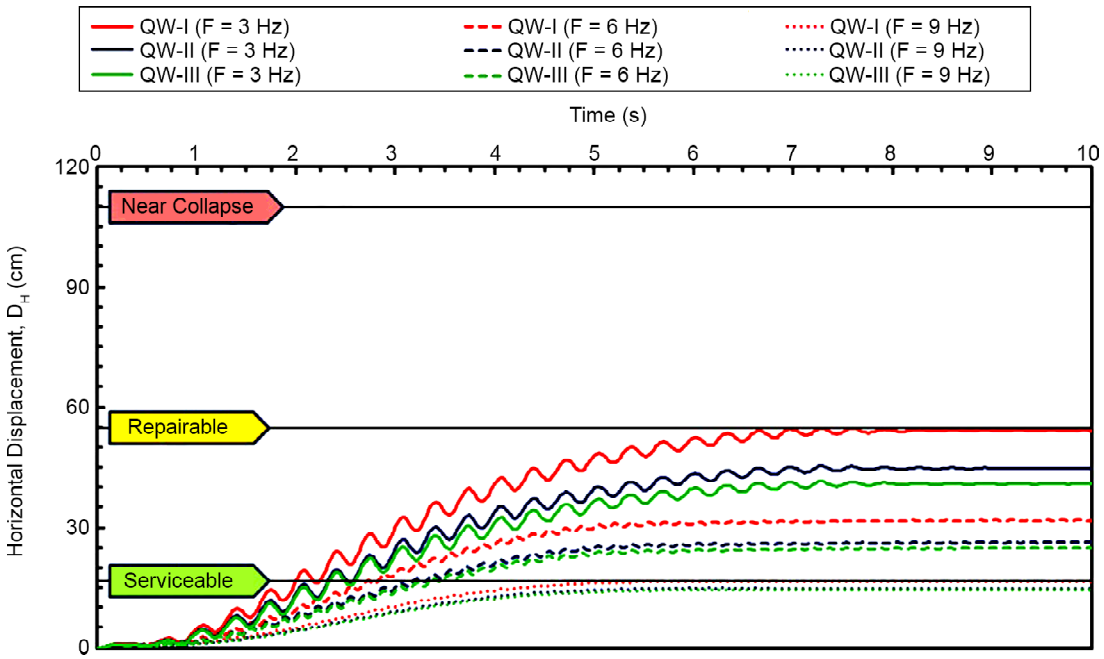

Figure 8. Horizontal displacement time histories of quay walls subjected to an input motion with a PGA = 0.6 g along with an indication of damage levels.

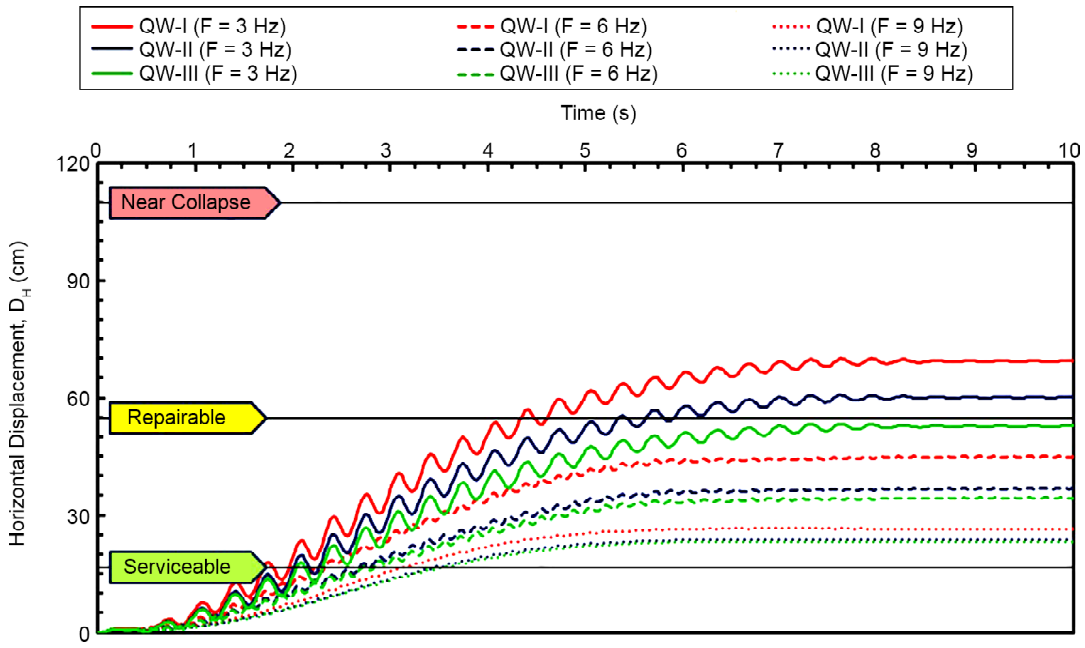

Figure 9. Horizontal displacement time histories of quay walls subjected to an input motion with a PGA = 0.9 g along with an indication of damage levels.

nificantly amplified responses. Lower-frequency seismic waves are more likely to match the natural frequencies of larger structures and deeper soil layers, causing more severe shaking and potential failure. As shown in Figure (3), the first mode of vibration of the QW-I, QW-II, and QW-III quay walls are the most actively participating mode in eigenvalue analysis with a natural frequency of approximately 2.97 Hz. Consequently, the most critical D_H of the quay walls occurs when the seismic load has a frequency of 3.0 Hz, as illustrated in Figures (6) to (9).

4.2. Dynamic Earth Pressure

The distinctive geometry of hunchbacked quay walls, characterized by their leaning slope and curved profile, significantly affects the distribution of lateral earth pressure acting on their backface. Unlike conventional vertical walls, the hunched shape alters the interaction between the backfill

material and the wall, resulting in distinct pressure patterns compared to vertical quay walls (Arablouei et al., 2011; Ebrahimian and Farboud, 2019; Yuksel et al., 2023; Chen et al., 2024a; Ko et al., 2024). Increasing the H_h from 3 m in the QW-I model to 5 m in the QW-II model and 6 m in the QW-III model raises the breaking point of the hunchbacked block quay wall.

The distribution of lateral earth pressure acting on the quay wall is influenced by the H_h. Figure (10) presents the distribution of dynamic pressure during different dynamic times of input motion, with a

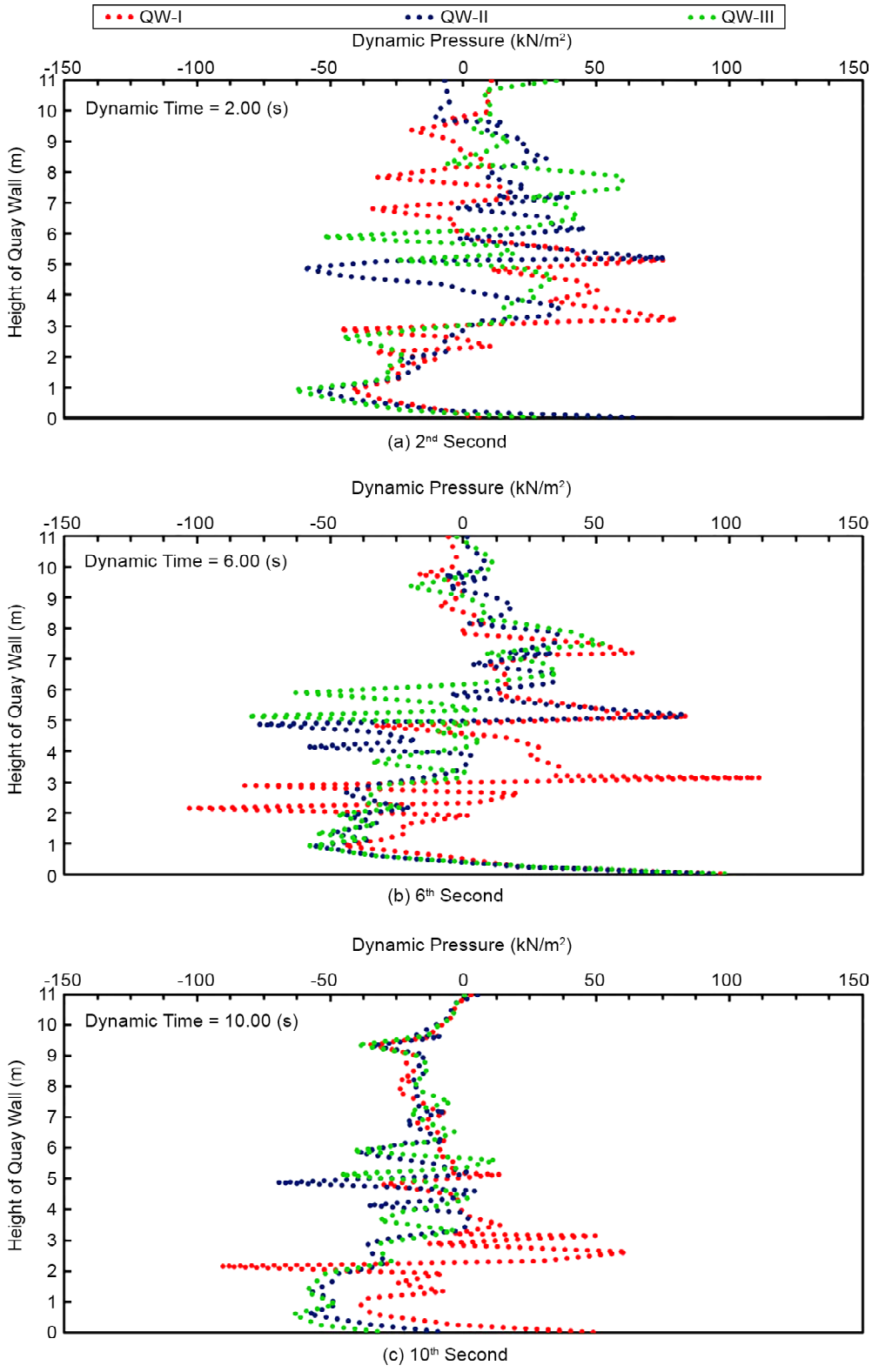

Figure 10. Distribution of dynamic pressures acting on the height of quay walls subjected to an input motion with a PGA = 0.9 g and f = 3 Hz.

PGA of 0.9g and a frequency of 3 Hz. During seismic loading, a higher H_h generally results in a reduction of lateral pressure. This decrease in force on the quay wall diminishes the tendency for D_H and enhances its stability. Conversely, a lower H_h can lead to increased lateral pressure acting on the back face of the quay wall, resulting in greater D_H. Based on the numerical results obtained, the backfill soil adjacent to the breaking point of the hunch in hunchbacked block-type quay walls ex-periences maximum lateral dynamic pressure acting on the wall at all time steps, as shown in Figure (10).

The dynamic pressure acting on the back face of quay walls is associated with the forces exerted by moving water and can fluctuate during seismic loading. Particularly during rapid changes in acceleration or deceleration, the dynamic pressure exerted on the quay wall can become negative, indicating a reduction in pressure relative to static conditions. This phenomenon can occur due to the fluid's inertial effects, where it may momentarily exert an upward force on the wall, resulting in a negative pressure reading. For example, during an earthquake, as the ground accelerates, the water's inertia can cause it to exert less pressure on the wall at certain points, potentially leading to negative dynamic pressures.

4.3. Backfill Settlement

Figure (11) illustrates the total displacement contours for the soil-quay wall system, revealing the formation of a failure wedge in the backfill soil. It is important to note that this behavior differs among the three types of quay walls. In the QW-I wall, which has a smaller H_h, the backfill behaves as a single failure wedge, exerting significant pressure that pushes the wall toward the sea. In

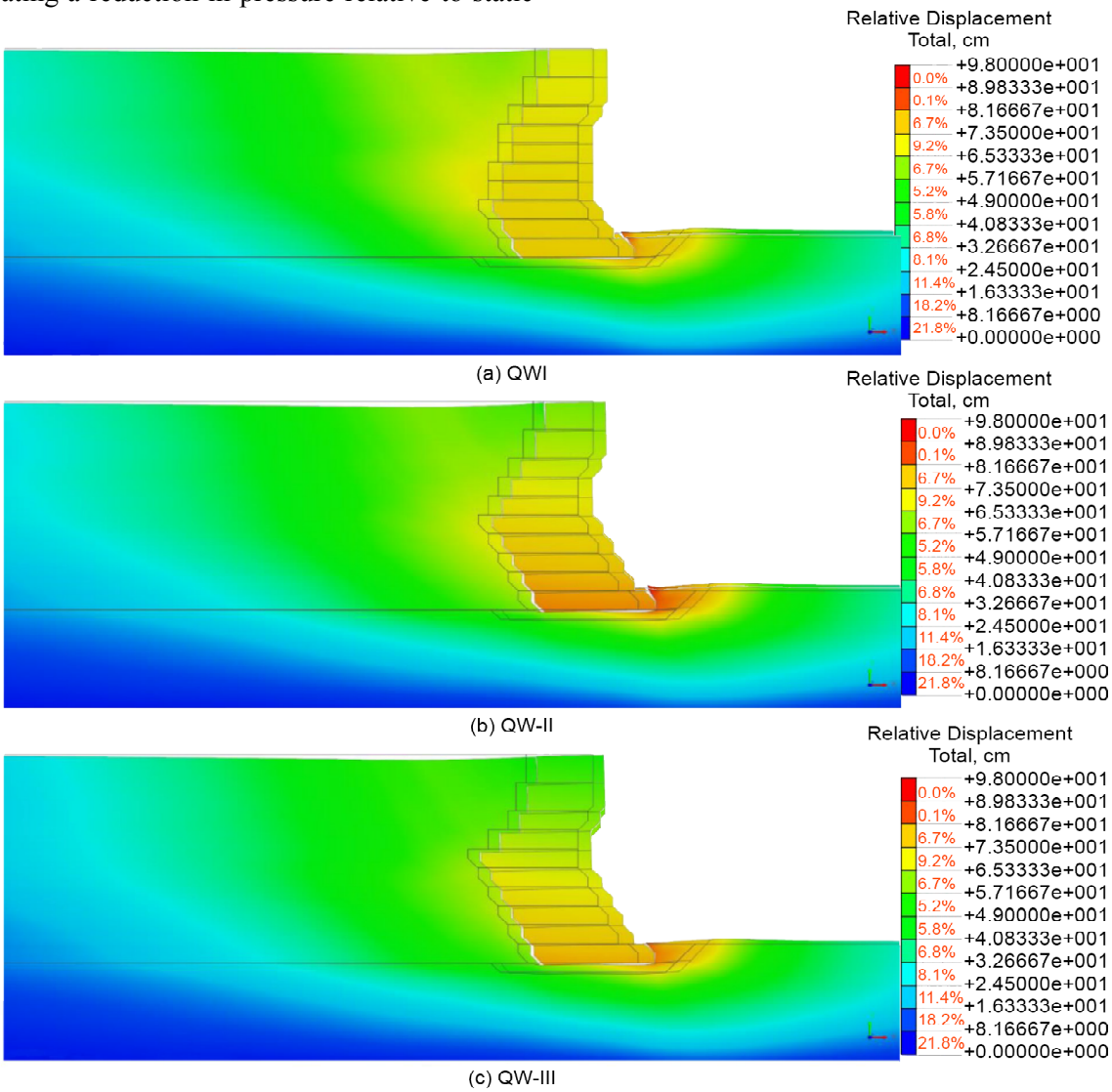

Figure 11. Post-earthquake total deformation of soil-quay wall system subjected to an input motion with a PGA = 0.9 g and f = 3 Hz.

contrast, the QW-II and QW-III walls exhibit a different response, where the backfill soil resting on the blocks moves in conjunction with the wall, resulting in the formation of a smaller failure wedge. Consequently, the backfill exerts greater lateral pressure on the QW-I model compared to the QW-II and QW-III models, as shown in Figure (10). Additionally, a lower angle θ_i increases the stability of the quay wall under seismic loads.

As illustrated in Figure (12), the maximum

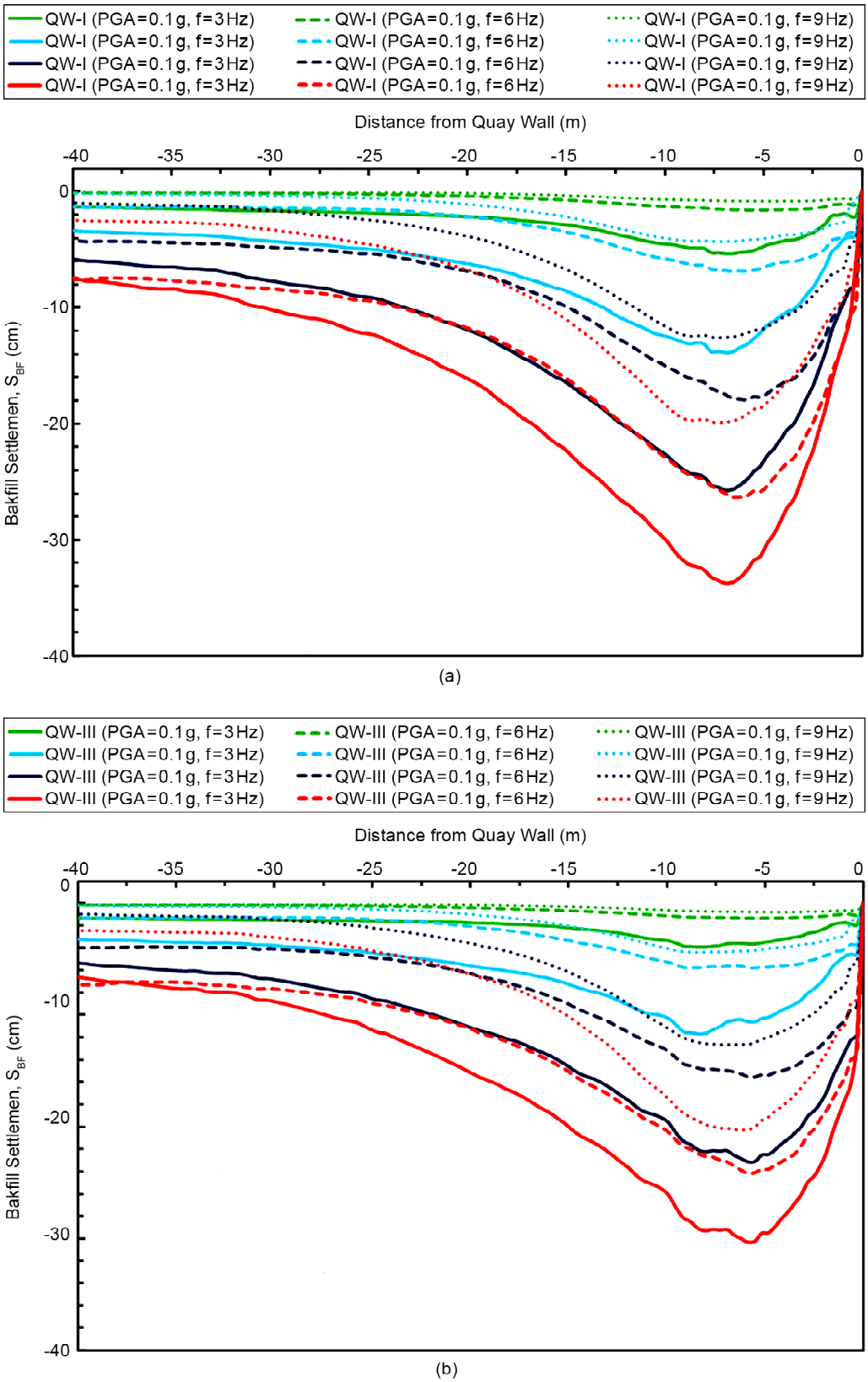

Figure 12. Settlement profile of backfill soil behind quay walls.

Table 2. Acceleration amplification on the surface of backfill soil behind quay wall.

Model	PGA (m/s^2)	Frequency (Hz)	Distance Measured from the Quay Wall				
			0.10 H	0.30 H	0.55 H	1.00 H	2.00 H
			Acceleration Amplification				
QW-I	9.0	3.0	1.80	1.64	1.46	1.39	1.36
QW-II			1.78	1.62	1.37	1.36	1.34
QW-III			1.52	1.41	1.33	1.30	1.28

settlement of the backfill (S_{BF}) does not occur immediately adjacent to the hunchbacked gravity quay walls. Instead, the settlement is observed within a range of 0.55 H to 0.65 H from the walls in the studied models. This finding is consistent with previous research conducted by Sadrekarimi (2011), Yuksel et al. (2017, 2023), and Baziar et al. (2020), which indicated that maximum backfill settlements typically occur at distances between 0.5 H and 1.0 H from the hunchbacked quay wall.

4.4. Acceleration

Table (4) displays the peak acceleration response ratios in relation to the input motion, with measurements taken at distances of 0.10 H, 0.30 H, 0.55 H, 1.00 H, and 2.00 H from the quay wall. The QW-I model demonstrates a maximum amplification of 1.80 at a distance of 0.10 H, while the QW-II and QW-III models show amplifications of 1.78 and 1.52, respectively, at the same distance. This pattern underscores the influence of quay wall geometry and hunch height on acceleration amplification, suggesting that an increase in hunch height results in reduced levels of acceleration amplification. The QW-III model is particularly less affected by seismic input motion, exhibiting lower acceleration amplification on the surface of the backfill soil, which translates to reduced horizontal displacement (Figure 9) and backfill settlement (Figure 12). Consequently, the QW-III model demonstrates better seismic performance compared to the QW-I and QW-II models.

5. Summary and Conclusion

This study investigates the effects of seismic loads characterized by peak ground accelerations ranging from 0.1 g to 0.9 g and frequencies from 3.0 Hz to 9.0 Hz on the seismic performance of quay walls while also examining variations in hunch height and upper inclination angle. Utilizing numerical finite element analysis with adaptive meshing strategies and interface elements, this research simulates discontinuities and models the interaction between the quay wall and the surrounding soil medium. The key findings indicate that quay wall displacement is directly proportional to input acceleration, with variations in PGA resulting in corresponding increases in horizontal displacements and backfill settlements. Additionally, increasing the input frequency at a constant acceleration level reduces seismic energy transfer, thereby minimizing horizontal displacements and backfill settlements. The study also reveals that increasing hunch height and optimizing the upper inclination angle can effectively lower lateral earth pressures and horizontal displacements, improving the quay wall's seismic performance. Finally, the results recommend maintaining a distance greater than the wall height (1.00 H) for optimal spacing between the quay wall and the construction of critical structures, infrastructure, and sensitive buildings in the backfill area, as maximum backfill settlement occurs within the range of 0.55 H to 0.65 H from the quay wall, posing risks to critical facilities, while acceleration amplification in the backfill significantly diminishes at distances greater than the wall height.

Abbreviations

FEM: Finite Element Method
FE: Finite Element
PGA: Peak Ground Accelerations
QW-I: Quay Wall type I
QW-II: Quay Wall type II
QW-III: Quay Wall type III
H: Quay wall height
L: Base block length
H_h: Hunch height
ω_i: Hunch angle
θ_i: Upper inclination angle
HS: Hardening soil model
HSsmall: Hardening soil model with small strain

G_0: Initial shear modulus
G_0^{ref} : Reference initial shear modulus at the reference pressure
P_{ref}: Reference pressure
G_s: Secant shear modulus
$\gamma_{0.7}$: Threshold shear strain
ξ: Damping ratio
α_R, β_R: Damping coefficients
ω_i, ω_j: The natural frequencies of vibration modes
E_D: Ratio of dissipated energy
E_S: Maximum strain energy
E_{ur}^{ref} : Loading-unloading stiffness
E_{50}^{ref} : Secant stiffness in drained triaxial test
E_{oed}^{ref} : Tangent stiffness for initial oedometer loading
k_n, k_t: Normal and shear stiffness modulus
R_{inter}: Resistance reduction factor
A' : Area of the interface between the quay wall and geo-materials
t_v: Virtual thickness of the interface
$E_{oed,i}$: Interface comparison modulus
G_{ur}: Average unloading-reloading shear modulus
D_H: Quay wall horizontal displacement
S_{BF}: Backfill settlement

References

Alielahi, H., & Moghadam, M. R. (2016). Fragility curves evaluation for hunchbacked block quay walls. *Journal of Earthquake Engineering*, *21*(1), 1-22. doi: 10.1080/13632469.2016.1142487

Alimoradi, H., Noorzad, A., & Ebrahimian, B. (2024). Explicit FE analysis of 3D failure envelopes of suction caisson foundations supporting offshore wind turbines in sand subjected to combined loading. *Ocean Engineering*, *301*, 116831. doi: 10.1016/j.oceaneng. 2024.116831

Alzabeebee, S., & Keawsawasvong, S. (2023). Dynamic response of a machine foundation using different soil constitutive models. *Transportation Infrastructure Geotechnology*, *11*(1), 426-445. doi: 10.1007/s40515-023-00284-4

Arablouei, A., Gharabaghi, A. R. M., Ghalandarzadeh, A., Abedi, K., & Ishibashi, I. (2011). Effects of seawater-structure-soil interaction on seismic performance of caisson-type quay wall. *Computers & Structures*, *89*(23-24), 2439-2459. doi: 10.1016/j.compstruc.2011.06.005

Augarde, C. E., Lee, S., & Loukidis, D. (2021). Numerical modelling of large deformation problems in geotechnical engineering: A state-of-the-art review. *Soils and Foundations*, *61*(6), 1718-1735. doi: 10.1016/j.sandf.2021.08.007

Bajaj, K., & Anbazhagan, P. (2019). Identification of shear modulus reduction and damping curve for deep and shallow sites: KIK-Net data. *Journal of Earthquake Engineering*, *25*(13), 2668-2696. doi: 10.1080/13632469.2019.1643807

Barron, J., Rouainia, M., Charlton, T., Edwards, S., & Gibson, F. (2024). Seismic performance of shared suction caisson anchors installed in liquefiable sand for floating offshore wind turbines. *Soil Dynamics and Earthquake Engineering*, *180*, 108598. doi: 10.1016/j.soildyn.2024.108598

Baziar, M. H., Sanaie, M., Amirabadi, O. E., Khoshniazpirkoohi, A., & Azizkandi, A. S. (2020). Mitigation of hunchbacked gravity quay wall displacement due to dynamic loading using shaking table tests. *Ocean Engineering*, *216*, 108056. doi: 10.1016/j.oceaneng.2020.108056

Calabrese, A., & Lai, C. G. (2016). Sensitivity analysis of the seismic response of gravity quay walls to perturbations of input parameters. *Soil Dynamics and Earthquake Engineering*, *82*, 55-62. doi: 10.1016/j.soildyn.2015.11.010

Cakir, T. (2013). Evaluation of the effect of earthquake frequency content on seismic behavior of cantilever retaining wall including soil-structure interaction. *Soil Dynamics and Earthquake Engineering*, *45*, 96-111. doi: 10.1016/j.soildyn. 2012.11.008

Chakraborty, D., & Choudhury, D. (2014). Sliding stability of non-vertical waterfront retaining wall supporting inclined backfill subjected to pseudo-dynamic earthquake forces. *Applied Ocean Research*, *47*, 174-182. doi: 10.1016/j.apor.2014. 05.004

Chen, S., Guo, W., & Ren, Y. (2024a). Numerical studies on the stability of caisson quay wall. *Ocean Engineering*, *296*, 116892. doi: 10.1016/j.oceaneng. 2024.116892

Chen, Z., Chen, G., & Liu, Y. (2024b). Effects of topographic irregularity on seismic site amplification considering input signal frequency: A case study. *Engineering Structures*, *304*, 117667. doi: 10.1016/j.engstruct.2024.117667

Chen, H., Chu, J., Guo, W., & Wu, S. (2022). Use of suction caissons for seawall construction. *Ocean Engineering*, *266*, 112632. doi: 10.1016/j.oceaneng.2022.112632

Cihan, H. K., Ergin, A., Cihan, K., & Guler, I. (2015). Dynamic responses of two blocks under dynamic loading using experimental and numerical studies. *Applied Ocean Research*, *49*, 72-82. doi: 10.1016/j.apor.2014.11.003

Cihan, H. K., & Cihan, K. (2021). Dynamic responses of block type quay walls under cyclic loading. *China Ocean Engineering*, *35*(2), 281-290. doi: 10.1007/s13344-021-0025-0

Coutinho, A. L. G. A., Martins, M. a. D., Sydenstricker, R. M., Alves, J. L. D., & Landau, L. (2003). Simple zero thickness kinematically consistent interface elements. *Computers and Geotechnics*, *30*(5), 347-374. doi: 10.1016/s0266-352x(03)00013-2

Dakoulas, P., Vazouras, P., Kallioglou, P., & Gazetas, G. (2018). Effective-stress seismic analysis of a gravity multi-block quay wall. *Soil Dynamics and Earthquake Engineering*, *115*, 378-393. doi: 10.1016/j.soildyn.2018.08.032

Ebrahimian, B., & Bauer, E. (2012). Numerical simulation of the effect of interface friction of a bounding structure on shear deformation in a granular soil. *International Journal for Numerical and Analytical Methods in Geomechanics*, *36*(12), 1486-1506. doi: 10.1002/nag.1059

Ebrahimian, B., Noorzad, A., & Alsaleh, M. I. (2012). Modeling shear localization along granular soil-structure interfaces using elasto-plastic Cosserat continuum. *International Journal of Solids and Structures*, *49*(2), 257-278. doi: 10.1016/j.ijsolstr.2011.09.005

Ebrahimian, B. (2013). Numerical modelling of the seismic behaviour of gravity-type quay walls. In: *D'Amico, S., Engineering Seismology, Geotechnical and Structural Earthquake Engineering*. InTech. doi: 10.5772/55027

Ebrahimian, B., & Bauer, E. (2014). Investigation of direct shear interface test using micro-polar continuum approach, in: Chau, K. T., Zhao, J., Bifurcation and Degradation of Geomaterials in the New Millennium. IWBDG 2014. *Springer Series in Geomechanics and Geoengineering*. Springer, 143-148. doi: 10.1007/978-3-319-13506-9_21

Ebrahimian, B., & Bahmani, S. (2019). Effect of liquefiable soil layer position on dynamic performance of anchored diaphragm walls-a numerical assessment. In *Proceeding of 8th International Conferences of Seismology and Earthquake Engineering* (*SEE8*), Tehran, Iran.

Ebrahimian, B., & Farboud, M. (2019). Seismic effective-stress analysis of caisson quay wall with liquefiable backfill. In *Proceeding of 8th International Conferences of Seismology and Earthquake Engineering (SEE8)*, Tehran, Iran.

Ebrahimian, B., & Panahi, A. H. (2019). Numerical evaluation of seismic behavior of rubble-mound breakwaters rested on a liquefiable seabed soil layer. In *Proceeding of 8th International Conferences of Seismology and Earthquake Engineering (SEE8)*, Tehran, Iran.

Ebrahimian, B., & Farahani, A. R. Z. (2023a). Mitigation of deformations of a hunchbacked block-type gravity quay wall subjected to dynamic loading through optimizing its back-face configuration, in: Mansouri, I., Awoyera, P., Seismic Evaluation, Damage, and Mitigation in Structures. *Woodhead Publishing Series in Civil and Structural Engineering*, 365-380. doi: 10.1016/b978-0-323-88530-0.00009-x

Ebrahimian, B., & Farahani, A. R. Z. (2023b). Developing seismic fragility curves for caisson-type quay walls with improved backfill soil, in: Mansouri, I., Awoyera, P., Seismic Evaluation, Damage, and Mitigation in Structures. *Woodhead Publishing Series in Civil and Structural Engineering*, 205-234. doi: 10.1016/b978-0-323-88530-0.00001-5

Ebrahimian, B., & Farahani, A. R. Z. (2024). Optimizing the geometry of hunchbacked block-type gravity quay walls using non-linear dynamic analy-

ses and supervised machine learning technique. *Sharif Journal of Civil Engineering*, *40*(1), 17-31 (in Persian). doi: 10.24200/j30.2023.61126.3150

Ehterami, A. A., Soltani Jigheh, H., & Rezaie Farie, A. H. (2022). Study on the parameters affecting rectifying asymmetric settlement of concrete building foundations by jacking method. *Sharif Journal of Civil Engineering*, *37.2*(1.2), 75-86 (in Persian). doi: 10.24200/j30.2020.55141.2705

Ehterami, A. A., Ebrahimian, B., & Noorzad, A. (2024). Numerical evaluation of deformation behavior of hunchbacked gravity quay walls subjected to dynamic loading. In *Proceeding of 9th International Conferences of Seismology and Earthquake Engineering (SEE9)*, Tehran, Iran.

Fatahi, B., Huang, B., Yeganeh, N., Terzaghi, S., & Banerjee, S. (2020). Three-dimensional simulation of seismic slope-foundation-structure interaction for buildings near shallow slopes. *International Journal of Geomechanics*, *20*(1). doi: 10.1061/(asce)gm.1943-5622.0001529

Gabor, D. (1946). Theory of communication. Part 1: the analysis of information. *Journal of the Institution of Electrical Engineers*, *93*(26), 429-441. doi: 10.1049/ji-3-2.1946.0074

Gazetas, G., Garini, E., & Zafeirakos, A. (2016). Seismic analysis of tall anchored sheet-pile walls. *Soil Dynamics and Earthquake Engineering*, *91*, 209-221. doi: 10.1016/j.soildyn.2016.09.031

Ghalandarzadeh, A., Rahimi, S., & Kavand, A. (2020). Dynamic pore water pressure of submerged backfill on caisson quay walls: 1g shake table tests. *Soil Dynamics and Earthquake Engineering*, *132*, 106091. doi: 10.1016/j.soildyn.2020.106091

Goyal, A., & Shrivastava, A. K. (2024). A novel heuristic and tunicate centered ANFIS and RCCRD optimization for soil nailing using a numerical approach. *Soil Dynamics and Earthquake Engineering*, *176*, 108289. doi: 10.1016/j.soildyn.2023.108289

Guo, W., Huang, J., Chen, S., & Ren, Y. (2023). Experimental study on the stability of L - Shaped hybrid quay wall in sand. *Ocean Engineering*, *280*, 114851. doi: 10.1016/j.oceaneng.2023.114851

Ha, S. J., and Kim, B. (2023). Responses of a cantilever retaining wall under multiple earthquake sequences. *Soil Dynamics and Earthquake Engineering*, *173*, 108116. doi: 10.1016/j.soildyn.2023.108116

Haukaas, T. (2024). Exact sensitivity of nonlinear dynamic response with modal and rayleigh damping formulated with the tangent stiffness. *Journal of Structural Engineering*, *150*(3). doi: 10.1061/jsendh.steng-12604

Hardin, B. D., & Drnevich, V. P. (1972). Shear modulus and damping in soils: Design equations and curves. *Journal of the Soil Mechanics and Foundations Division*, *98*(7), 667-692. doi: 10.1061/jsfeaq.0001760

Iai, S. (2019). Evaluation of performance of port structures during earthquakes. *Soil Dynamics and Earthquake Engineering*, *126*, 105192. doi: 10.1016/j.soildyn.2018.04.055

Ishihara, K., Yasuda, S., & Nagase, H. (1996). Soil characteristics and ground damage. *Soils and foundations*, *36*(Special), 109-118. doi: 10.3208/sandf.36.Special_109

Jafarian, Y., & Miraei, M. (2019). Scalar- and Vector-Valued Fragility analyses of gravity quay wall on liquefiable soil: example of Kobe Port. *International Journal of Geomechanics*, *19*(5). doi: 10.1061/(asce)gm.1943-5622.0001382

Jimenez, G. a. L., Dias, D., & Jenck, O. (2019). Effect of layered liquefiable deposits on the seismic response of soil-foundations-structure systems. *Soil Dynamics and Earthquake Engineering*, *124*, 1-15. doi: 10.1016/j.soildyn.2019.05.026

Kardani, M., Nazem, M., Abbo, A. J., Sheng, D., & Sloan, S. W. (2011). Refined h-adaptive finite element procedure for large deformation geotechnical problems. *Computational Mechanics*, *49*(1), 21-33. doi: 10.1007/s00466-011-0624-3

Khosrojerdi, M., & Pak, A. (2015). Numerical investigation on the behavior of the gravity waterfront structures under earthquake loading. *Ocean Engineering*, *106*, 152-160. doi: 10.1016/j.oceaneng.2015.07.003

Ko, Y., Yang, H., Hu, C., Huang, Y., & Lin, Y. (2024). Numerical seismic performance assessment and fragility analysis for gravity-type wharves considering the influence of soil liquefaction. *Soil Dynamics and Earthquake Engineering*, *180*, 108581. doi:10.1016/j.soildyn.2024.108581

Lee, C. (2005). Centrifuge modeling of the behavior of caisson-type quay walls during earthquakes. *Soil Dynamics and Earthquake Engineering*, *25*(2), 117-131. doi: 10.1016/j.soildyn.2004.10.011

Lee, M., Sun, C., Cho, H., Kim, H., & Ha, J. (2022). Experimental study on seismic response of gravity-type quay wall considering input earthquake frequency and excess pore pressure buildup in backfill. *Ocean Engineering*, *257*, 111667. doi: 10.1016/j.oceaneng.2022.111667

Li, Y., & Mo, P. (2019). A unified landslide classification system for loess slopes: A critical review. *Geomorphology*, *340*, 67-83. doi: 10.1016/j.geomorph.2019.04.020

Liu, C., Weng, J., Deng, L., Wang, Y., & Fang, Q. (2024). Numerical investigation of phase relationship between kinematic and inertial loads of piles behind a quay wall in liquefiable ground. *Computers and Geotechnics*, *170*, 106265. doi: 10.1016/j.compgeo.2024.106265

Mezeh, R., Sadek, M., Chehade, F. H., Mroueh, H. (2018). Adaptive meshing scheme for prediction of high-speed moving loads induced ground vibrations. *Computers and Geotechnics*, *100*, 188-202. doi: 10.1016/j.compgeo.2018.03.014

MIDAS IT. Co. Ltd. (2021). *MIDAS GTS NX user manual. MIDAS Information Technology Co., Ltd*, 1-567. https://globalsupport.midasuser.com/helpdesk/KB/View/32636343-midas-gts-nx-manuals-and-tutorials

Moghadam, A. M., Ghalandarzadeh, A., Towhata, I., Moradi, M., Ebrahimian, B., & Hajialikhani, P. (2009). Studying the effects of deformable panels on seismic displacement of gravity quay walls. *Ocean Engineering*, 36(15-16), 1129-1148. doi: 10.1016/j.oceaneng.2009.08.006

Moghadam, A. M., Ghalandarzadeh, A., Moradi, M., Towhata, I., & Hajialikhani, P. (2011). Displacement reducer fuses for improving seismic performance of caisson quay walls. *Bulletin of Earthquake Engineering*, 9(4), 1259-1288. https://doi.org/10.1007/s10518-011-9250-x

Mroginski, J. L., & Etse, G. (2013). A finite element formulation of gradient-based plasticity for porous media with C1 interpolation of internal variables. *Computers and Geotechnics*, *49*, 7-17. doi: 10.1016/j.compgeo.2012.11.003

Najma, A., & Ghalandarzadeh, A. (2019). Experimental study on the seismic behavior of composite breakwaters located on liquefiable seabed. *Ocean Engineering*, *186*, 106127. doi: 10.1016/j.oceaneng.2019.106127

Niu, Y., Cheng, Y., Li, J., Wang, X., He, K., Zhang, Z., & Ding, X. (2024). Research on bearing behaviour of buried double corrugated steel culvert with high fill considering spacing effect. *Case Studies in Construction Materials*, *20*, e02943. do: 10.1016/j.cscm.2024.e02943

Onyelowe, K. C., Ebid, A. M., Sujatha, E. R., Fazel-Mojtahedi, F., Golaghaei-Darzi, A., Kontoni, D. N., & Nooralddin-Othman, N. (2023). Extensive overview of soil constitutive relations and applications for geotechnical engineering problems. *Heliyon*, *9*(3), e14465. doi: 10.1016/j.heliyon.2023.e14465

PIANC (Permanent International Association of Navigation Congresses). (2001). *Seismic Design Guidelines for Port Structures*. Brussels: PIANC General Secretariat - Maritime Navigation Commission. Working Group No. 34, Brussels, Belgium.

Radampola, S., Gurung, N., McSweeney, T., & Dhanasekar, M. (2008). Evaluation of the properties of railway capping layer soil. *Computers and Geotechnics*, *35*(5), 719-728. doi: 10.1016/j.compgeo.2008.01.001

Rezaie Farie, A. H., & Ehterami, A. A. (2018). Study of Mechanized Tunnel Boring Machines Performance in Urban Areas. *New Approaches in Civil Engineering*, *1*(2), 14-30 (in Persian). doi: 10.30469/jnace.2018.63077

Rezaei Farei, A., & Ehterami, A. A. (2019). Surface Buildings risk classification and evaluation of

in-situ piles effect in mitigation the settlements caused by excavation of metro tunnels in urban areas (Case Study). *Journal of Transportation Infrastructure Engineering*, *5*(1), 97-119 (in Persian). doi: 10.22075/jtie.2018.13548.1278

Sadrekarimi, A., Ghalandarzadeh, A., & Sadrekarimi, J. (2008). Static and dynamic behavior of hunch-backed gravity quay walls. *Soil Dynamics and Earthquake Engineering*, *28*(2), 99-117. doi: 10.1016/j.soildyn.2007.05.004

Sadrekarimi, A. (2011). Seismic displacement of Hunchbacked gravity quay walls. *Journal of Waterway, Port, Coastal, and Ocean Engineering*, *137*(2), 75-84. doi: 10.1061/(asce)ww.1943-5460.0000066

Sadrekarimi, A. (2012). Dynamic behavior of granular soils at shallow depths from 1 g shaking table tests. *Journal of Earthquake Engineering*, *17*(2), 227-252. doi: 0.1080/13632469.2012.691616

Sandoval, E., & Bobet, A. (2020). Effect of input frequency on the seismic response of deep circular tunnels. *Soil Dynamics and Earthquake Engineering*, *139*, 106421. doi: 10.1016/j.soildyn.2020.106421

Santhoshkumar, G. (2020). Seismic stability analysis of a hunchbacked retaining wall under passive state using method of stress characteristics. *Acta Geotechnica*, *15*(10), 2969-2982. doi: 10.1007/s11440-020-01003-w

Savigamin, C., & Bobet, A. (2024). Seismic response of deep circular tunnels subjected to P-waves: axial and transverse compression-extension. *Soil Dynamics and Earthquake Engineering*, *176*, 108338. doi: 10.1016/j.soildyn.2023.108338

Seed, H. B., Wong, R. T., Idriss, I. M., & Tokimatsu, K. (1986). Moduli and damping factors for dynamic analyses of cohesionless soils. *Journal of Geotechnical Engineering*, *112*(11), 1016-1032. doi: 10.1061/(asce)0733-9410(1986)112:11(1016)

Shabani, M. J., Shamsi, M., & Zakerinejad, M. (2022). Slope topographic impacts on the nonlinear seismic analysis of soil-foundation-structure interaction for similar MRF buildings. *Soil Dynamics and Earthquake Engineering*, *160*, 107365. doi: 10.1016/j.soildyn.2022.107365

Shekari, M. R. (2023). Numerical study on response characteristics of a caisson-type quay wall subjected to bidirectional ground shaking. *Ocean Engineering*, *273*, 113639. doi: 10.1016/j.oceaneng.2023.113639

Soltani-Jigheh, H., & Ehterami, A. A. (2024). Numerical investigation of jacking method for asymmetric settlement rectification in tilted concrete buildings. *Case Studies in Construction Materials*, *20*, e02710. doi: 10.1016/j.cscm.2023.e02710

Stelzer, R. S., & Hofstetter, G. (2005). Adaptive finite element analysis of multi-phase problems in geotechnics. *Computers and Geotechnics*, *32*(6), 458-481. doi: 10.1016/j.compgeo.2005.06.003

Sugano, T., Nozu, A., Kohama, E., Shimosako, K., & Kikuchi, Y. (2014). Damage to coastal structures. *Soils and Foundations*, *54*(4), 883-901. doi: 10.1016/j.sandf.2014.06.018

Tasiopoulou, P., Gerolymos, N., & Gazetas, G. (2015). CLASS Class A prediction for seismic centrifuge modeling of multi-block quaywall: Undrained (PLAXIS) versus coupled (FLAC) effective stress analysis. In *Proceedings of 5th ECCOMAS Thematic Conf. on Computational Methods in Structural Dynamics and Earthquake Engineering: European Community on Computational Methods in Applied Sciences*. Spain, Barcelona. doi: 10.7712/120115.3578.1577

Timuragaoglu, M. O. (2024). Kinematic interaction analysis of individual soil-pile model within multi-block system. *Soil Dynamics and Earthquake Engineering*, *179*. doi: 10.1016/j.soildyn.2024.108523

Tiznado, J. C., & Rodriguez-Roa, F. (2011). Seismic lateral movement prediction for gravity retaining walls on granular soils. *Soil Dynamics and Earthquake Engineering*, *31*(3), 391-400. doi: 10.1016/j.soildyn.2010.09.008

Tong, B., & Schaefer, V. R. (2016). Optimization of vibrocompaction design for liquefaction mitigation of gravity caisson quay walls. *International Journal of Geomechanics*, *16*(4). doi: 10.1061/(asce)gm.1943-5622.0000585

Tong, B., Schaefer, V., Liu, Y., & Han, B. (2018). Optimization of deep mixing design for seismic

liquefaction mitigation of Caisson walls. *Geomatics, Natural Hazards and Risk*, *10*(1), 287-313. doi: 10.1080/19475705.2018.1521879

Towhata, I. (2021). Liquefaction mitigation measures: a historical review, in: Sitharam, T., Jakka, R., Kolathayar, S., latest developments in geotechnical earthquake engineering and soil dynamics. *Springer Transactions in Civil and Environmental Engineering*. Springer, Singapore. doi: 10.1007/978-981-16-1468-2_3

Xiao, Z., Xie, S., Hu, A., Chen, Y., & Wang, M. (2024). Displacement control in irregular deep excavation adjacent to tunnel groups in structural soil: a case study of MJS cement-soil composite piles and grouting rectification. *Case Studies in Construction Materials*, *20*, e03085. doi: 10.1016/j.cscm.2024.e03085

Yu, Y., Damians, I. P., & Bathurst, R. J. (2015). Influence of choice of FLAC and PLAXIS interface models on reinforced soil-structure interactions. *Computers and Geotechnics*, *65*, 164-174. doi: 10.1016/j.compgeo.2014.12.009

Yuksel, Y., Yuksel, Z. T., Çevik, E., Orhan, K., & Berilgen, M. (2017). Evaluation of the seismic performance of a caisson and an L-type quay wall. *Soil Dynamics and Earthquake Engineering*, *92*, 537-550. doi: 10.1016/j.soildyn.2017.08.002

Yuksel, Z. T., Gerolymos, N., & Yuksel, Y. (2023). On the seismic performance of block type quay walls: Numerical analyses against 1g shaking tank tests. *Ocean Engineering*, *281*, 114942. doi: 10.1016/j.oceaneng.2023.114942

Zalachoris, G., Zekkos, D., Athanasopoulos-Zekkos, A., & Gerolymos, N., (2021). The role of liquefaction on the seismic response of quay walls during the 2014 Cephalonia, Greece, earthquakes. *Journal of Geotechnical and Geoenvironmental Engineering*, *147*(12). doi: 10.1061/(asce)gt.1943-5606.0002662

Zhang, Z., Li, J., & Ni, F. (2022). Material innovation preparation and performance study of semi-flexible pavement materials. *Case Studies in Construction Materials*, *17*, e01355. doi: 10.1016/j.cscm.2022.e01355